

Structure and atomic interactions at the Co/Pd(001) interface: Surface x-ray diffraction and atomic-scale simulations

H. L. Meyerheim,* V. Stepanyuk, A. L. Klavsyuk, E. Soyka, and J. Kirschner
Max-Planck-Institut für Mikrostrukturphysik, Weinberg 2, D-06120 Halle, Germany

(Received 8 June 2005; revised manuscript received 13 July 2005; published 9 September 2005)

Using surface x-ray diffraction and atomic-scale simulations we have studied the structure of Co films deposited on Pd(001) at room temperature by thermal (TD) and pulsed laser deposition (PLD). While for TD we find epitaxial growth of Co without sizable amount of intermixing, for PLD films substantial alloying is observed. *Ab initio* calculations indicate an oscillatory Co-Co interaction in the Pd layers, which is repulsive for nearest neighbors and attractive for next-nearest neighbors.

DOI: [10.1103/PhysRevB.72.113403](https://doi.org/10.1103/PhysRevB.72.113403)

PACS number(s): 68.35.Ct, 61.10.-i, 75.70.Ak

Since the physical properties of ultrathin films are intimately related to subtle details of the geometric structure, low-dimensional systems are intensely studied where structures can be prepared, which do not exist in the bulk. For instance, epitaxial ultrathin films often adopt a crystal structure imposed by the substrate crystal. A prominent example is fcc-Fe grown on Cu(001), where a number of different magnetic structures [ferromagnetic (FM), antiferromagnetic (AFM) or spiral structures] have been proposed.¹⁻³

On the other hand, intermixing between adsorbate and substrate leads to surface alloys, where two classes can be distinguished: First, the surface alloy is composed of components immiscible in the bulk.⁴ Examples are Mn/Cu(001) and Au/Ni(110).^{5,6} The second class of alloys consists of components, which are miscible within a wide range of compositions. Surface alloys of this kind are metastable systems far from their thermodynamic minimum.

The binary CoPd system represents an example of the latter, where a continuous solid solution over the whole composition range exists and well defined ordered phases are known.⁷ Ultrathin Co-Pd alloys are also of particular interest in magnetic storage device technology due to their ability to exhibit perpendicular magnetic anisotropy. Thus, a number of studies on the growth of Co on Pd(001) were carried out in the past.⁸⁻¹¹

For preparation of ultrathin films it is a common approach to deposit films by thermal deposition (TD), where the metal is evaporated from a heated rod. In contrast, only a few studies have been carried out using pulsed laser deposition (PLD) to prepare ultrathin films. A review is given by Shen *et al.*¹²

In general, improved epitaxy of PLD-grown films is attributed to both, the 4–6 orders of magnitude higher instantaneous deposition rate and the higher kinetic energy (up to several eV) of the deposited atoms, which are the main characteristics of PLD.^{12,13}

While several examples indicate the potential of PLD to have substantial impact on growth, morphology and magnetism of ultrathin films,¹⁴⁻¹⁶ the analysis of the atomic structure of PLD grown films is largely unexplored and only one quantitative low-energy electron diffraction analysis exists.¹⁷ To this end we have carried out a surface x-ray diffraction (SXRD) structure analysis of Co adlayers deposited on Pd(001) by using both, TD and PLD. In contrast to TD de-

posited films, where we find epitaxial growth of Co without significant alloying, for PLD deposited films a nonstoichiometric interface $\text{Co}_x\text{Pd}_{1-x}$ alloy extending over several layers is formed. Atomic-scale simulations and *ab initio* calculations confirm the experimental results indicating that the thickness of the alloyed interface sensitively depends on the kinetic energy of the deposited atoms.

Experiments were carried out in a UHV-system using a z -axis diffractometer setup for the SXRD data collection.¹⁸ The Pd(001) crystal was cleaned by standard methods (Ar⁺-ion sputtering followed by annealing at 900 K) until no traces of contaminants could be observed by Auger-electron spectroscopy (AES). Co was deposited by TD using a Co rod heated by electron bombardment. For PLD, a KrF excimer laser (248 nm wavelength, 34 ns pulse length, repetition rate 10 Hz, pulse energy ≈ 325 mJ) was focused on a Co target about 120 mm away from the sample surface. An average deposition rate between 0.1 and 0.3 monolayers (ML) per min. is achieved comparable to the deposition rate for TD. We refer to 1 ML as one adatom per substrate atom, i.e., 1.32×10^{15} atoms/cm². In all cases the sample was kept at room temperature.

X rays were generated by a rotating anode system and monochromatized (Cu- $K\alpha$ radiation) by using a multilayer optics yielding a peak count rate in the range of several hundred cts./sec at the antiphase condition of a crystal truncation rods (CTR's).^{19,20} Integrated x-ray reflection intensities were collected under total reflection conditions of the incoming beam (incidence angle $\alpha_i \approx 0.32^\circ$) by rotating the sample about its surface normal.^{19,20} In total, seven different data sets in the coverage range between about 0.4 and 3.3 ML were collected, two of them after TD, five after PLD deposition.

As a representative example, Fig. 1 shows the structure factor amplitudes $|F|$ along the (10 ℓ) and the (11 ℓ) (Ref. 22) CTR measured up to $q_z = 1.8$ reciprocal lattice units (rlu). The normal momentum transfer (q_z) is given by $q_z = \ell \times c^*$, where $c^* = 1.61 \text{ \AA}^{-1}$ is the rlu of Pd along q_z . The coordinate ℓ is continuous due to the crystal truncation.²¹ The $|F|$'s were derived from the integrated intensities after correcting the data for geometric factors.²³

For each data set, four symmetry independent CTR's [(10 ℓ), (11 ℓ), (20 ℓ), and (21 ℓ)] were collected correspond-

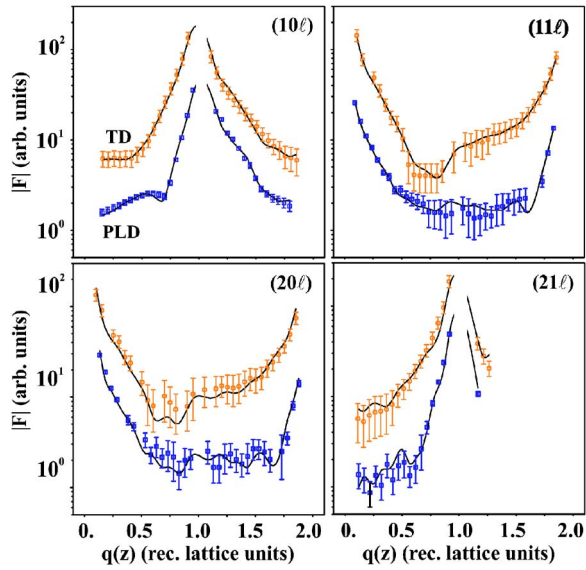


FIG. 1. (Color online) Measured (symbols) and calculated (lines) structure factor amplitudes along the (10ℓ) , (11ℓ) , (20ℓ) , and (21ℓ) crystal truncation rods for Co/Pd(001) prepared by PLD (lower curves, blue squares) and TD (upper curves, red circles). Curves are shifted for clarity.

ing to about 120 independent reflections. Standard deviations of the $|F|$'s were derived from the counting statistics and the reproducibility of symmetry equivalent reflections.^{19,20} Squares and circles correspond to data collected for samples prepared by PLD (lower curves) and TD (upper curves) at about the same coverage (TD: ≈ 1.4 ML, PLD: ≈ 1.2 ML). Direct comparison reveals significant differences between the samples. The quantitative structure analysis was carried out by least square refinement of the calculated $|F|$'s to the experimental ones.

Due to the high plane group symmetry ($p4mm$) and the simple structure there is only one independent atomic in-plane position per layer located either at $(0,0)$ or $(1/2, 1/2)$ within the two-dimensional unit cell. Therefore, apart from an overall scale factor only one z parameter is to be refined for each layer. Different alloy compositions are simulated by varying the Co (Θ_{Co}) and Pd (Θ_{Pd}) site occupancy, where $\Theta_{\text{Co}} + \Theta_{\text{Pd}} = 1$ in the case of complete layers. For modeling the structure in total only about ten parameters are needed, which in comparison with the number of data points (≈ 120) is a number low enough to ensure a sufficient over determination of the refinement problem.

Very good fits as represented by the solid lines could be achieved. The fit quality is measured by the un-weighted residuum (R_u) and the goodness of fit (GOF) parameter, the latter also taking into account the difference between the number of data points and the number of parameters.²⁴ Excellent values in the range between $R_u = 0.06 - 0.08$ and $\text{GOF} \approx 1$ were achieved in general.

A pictorial side view of the structure models is displayed in Fig. 2(a). Blue (dark) and grey (bright) balls represent Co and Pd atoms, respectively. In order to clarify the alloy

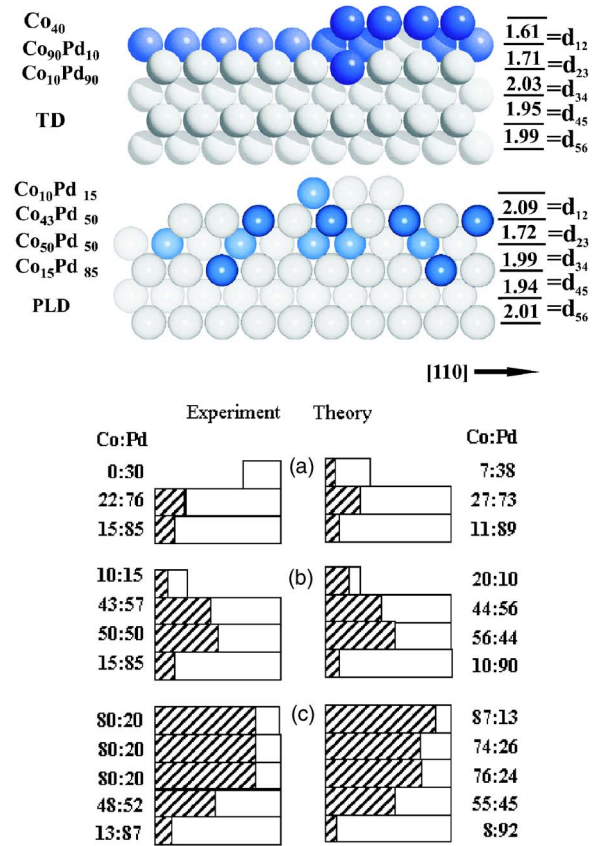


FIG. 2. (Color online) (a) SXR D derived structure model for Co/Pd(001) deposited by TD (upper panel) and PLD (lower panel). Blue (dark) and grey (bright) balls represent Co and Pd atoms, respectively. Alloy compositions within each layer are given on the left, inter layer distances in Å are listed on the right. (b) Experimental (left) and calculated (right) layer resolved Co concentration in PLD grown samples for 0.40 (α), 1.40 (β), and 3.00 ML (γ). Hatched and empty bars represent the Co and Pd concentrations

concentration within the layers, several unit cells along the $[110]$ direction are shown. In each layer, the corresponding number of Co and Pd atoms is placed according to the refined alloy concentration. No superstructure reflections were observed, therefore the alloys are random preserving the overall (1×1) -lattice periodicity of the Pd(001) substrate. This is also confirmed by the calculations discussed below.

For the sample prepared by TD we find no indication for alloying to within 10% of a ML, which is about the accuracy limit for the concentration determination. Instead, we find that face centered tetragonal (fct) Co grows epitaxially in a layer-by-layer mode on the Pd(001) surface. Apart from the fact that different structures and morphologies such as, e.g., island formation can be excluded by the SXR D analysis, layer-by-layer growth is also evidenced by reflection high-energy electron diffraction and scanning tunneling microscopy experiments, which will be published elsewhere.²⁷

Our structure model is at some variance with previous studies on Co and Fe layers on Pd(001), where intermixing has been found.^{10,11,25,26} We tentatively attribute this to different preparation conditions. Mild annealing of the

as-deposited TD samples [350 K for Fe/Pd(001) and 600 K for Co/Pd(001)] leads to the onset of alloy formation.²⁷

For the topmost Co-interlayer spacing (d_{12}) we determine 1.61(10) Å, which is 10% less than the fcc-bulk spacing of 1.77 Å. In agreement with elasticity theory considerations,⁹ the contraction can be related to the 10% in-plane expansion of the Co structure to adapt to the Pd lattice (lattice constants: 2.50 Å for Co vs 2.75 Å for Pd).

It is well known that hydrogen is often present on the Pd(001) surface and induces a significant expansion of d_{12} of the order of several percent.^{28,29} The measured value of d_{12} for the Co-covered sample does not provide any evidence that hydrogen is still present and influences the top layer spacing. Rather, we may speculate, that hydrogen might be displaced into the interior of the sample upon Co deposition. This is supported by significantly enhanced measured layer spacings (>2.00 Å) between the topmost Pd layers, which are not alloyed with Co [e.g., d_{34} for the TD and d_{56} for the PLD].

In sharp contrast to TD, for PLD alloy formation extending over several layers is observed in general. As shown in Fig. 2(a), four layers are affected in the case of the 1.2 ML sample. The left part of Fig. 2(b) summarizes the experimentally derived concentration profiles of the samples covered by approximately 0.4(α), 1.2(β), and 3.0 ML(γ). At low coverage, Co can be viewed as an impurity within the Pd-matrix, while almost pure Co adlayers (80%) are formed after deposition of 3 ML. The crossover between the two regimes lies at about 1.4 ML, where the Co concentration equals about 50% in the second and third layer.

Atomic scale simulations were carried out to calculate the alloy profiles. The simulation cell representing the (100) oriented Pd crystal consists of 11 layers containing 1250 atoms per layer. Two bottom layers are kept fixed and periodic boundary conditions are applied along the two directions of the surface plane. The interaction between atoms is described by the many-body *ab initio* fitted potentials formulated in the framework of the second moment approximation of the tight-binding (TB) model.^{30,31} The Kohn Korringa Rostoker (KKR) Green's functions calculations³² of binding energies of small Co clusters (dimer, trimer, pentamer), the atomic Co chains (3–5 atoms) on the Pd(001) surface, and the interaction energies between embedded Co impurities at different distances have been used to accurately fit the parameters of the interactions at the Co/Pd(001) interface.³³

Total energy calculations performed using the KKR Green's function method indicate that in the case of Co/Pd(001) alloy formation is favored. The energy gain induced by exchange of a single Co adatom with a top-layer Pd atom equals -0.42 eV as compared to Co-surface adsorption, but there is a kinetic exchange barrier of 0.4 eV. Therefore, only for samples grown by PLD alloy formation is observed. In contrast, for TD epitaxial growth is observed at RT and alloy formation requires annealing to overcome the barrier.²⁷

The right panel of Fig. 2(b) shows the calculated alloy concentrations. In general, very good agreement with the experimental data is observed. A prerequisite is the proper choice of the kinetic energy of the arriving Co atoms, which was set to 4 eV.

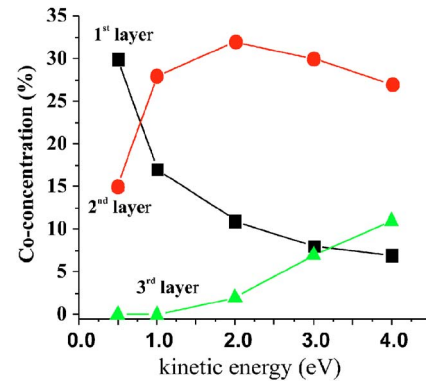


FIG. 3. (Color online) Calculated layer resolved Co concentration in percent as a function of the kinetic energy of the Co atoms for 0.45 ML Co/Pd(001).

The energy dependence of the Co-concentrations is shown in more detail in Fig. 3 for the low coverage sample. Significant alloying of the third layer requires an energy above about 2 eV. Simultaneously, with increasing energy the topmost layer is considerably depleted in Co, which is mostly transferred into the second layer.

Finally, we consider the interaction of two Co atoms in the Pd surface at short and intermediate distances. Our *ab initio* results presented in Fig. 4 show that the interaction energy is oscillatory. Negative and positive energies correspond to attraction and repulsion, respectively. While the interaction for the nearest-neighbor (NN) dimers of Co is strongly repulsive, the interaction for the next-NN (NNN) sites is attractive. It was shown by Hoshino *et al.*³⁴ that the fundamental characteristic features of the phase diagrams can be qualitatively explained by the NN interaction of atom pairs. The attractive interaction leads to segregation, the repulsive one to a solid solution. Our finding indicates that at low coverages a random distribution of isolated Co impurities in the Pd surface is energetically favorable. A small attractive interaction between the two Co impurities around 4 Å may play an important role only at very low temperatures leading to the dimer formation on the NNN sites. With increasing temperature the energy of Co impurities will be sufficient to overcome the repulsive barrier around 6 Å and Co dimers on the NNN sites will be destroyed. Presumably

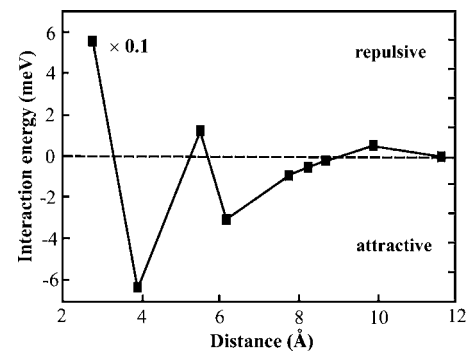


FIG. 4. Calculated interaction energy versus Co-interatomic distance.

metastable Co dimers on the NN sites can be formed in the PLD experiments due to a rather large thermal energy of incoming Co atoms.

In summary, we have studied the structure of the Co/Pd(001) interface prepared by TD and PLD. While an epitaxial fct-Co layer grows on Pd(001) in the case of TD, substantial alloying is observed for PLD. Atomic scale simu-

lations fairly well reproduce the experimentally derived alloy concentrations. Within the alloy layers, the Co-Co interaction shows an oscillating behavior, which is repulsive for nearest neighbors and attractive for next-nearest neighbors.

The authors acknowledge the technical support of W. Greie during the experiments.

*Electronic address: hmeyerhm@mpi-halle.mpg.de

- ¹J. Thomassen, F. May, B. Feldmann, M. Wuttig, and H. Ibach, *Phys. Rev. Lett.* **69**, 3831 (1991).
- ²D. Li, M. Freitag, J. Pearson, Z. Q. Qiu, and S. D. Bader, *Phys. Rev. Lett.* **72**, 3112 (1994).
- ³D. Qian, X. F. Jin, J. Barthel, M. Klaua, and J. Kirschner, *Phys. Rev. Lett.* **87**, 227204 (2001).
- ⁴J. Tersoff, *Phys. Rev. Lett.* **74**, 434 (1995)
- ⁵M. Wuttig, Y. Gauthier, and S. Blügel, *Phys. Rev. Lett.* **70**, 3619 (1992).
- ⁶L. Pleth, I. Stensgaard, E. Laegsgaard, and F. Besenbacher, *Surf. Sci.* **307**, 544 (1994).
- ⁷B. Predel, *Phase Equilibria, Crystallographic and Thermodynamic Data of Binary Alloys*, Landolt-Börnstein, Numerical Data and Functional Relationships in Science and Technology, New Series, Group IV: Macroscopic Properties of Matter, Vol. 5 (Springer, Berlin, 1993).
- ⁸P. F. Garcia, A. D. Meinhalt, and A. Suna, *Appl. Phys. Lett.* **47**, 178 (1985).
- ⁹H. Giordano, A. Atrei, M. Torrini, and U. Bardi, *Phys. Rev. B* **54**, 11 762 (1996)
- ¹⁰S.-K. Kim and S.-C. Shin, *J. Appl. Phys.* **89**, 3055 (2001)
- ¹¹J. T. Kohlepp, G. J. Strijkers, H. Wieldraaijer, and W. J. M. de Jonge, *Phys. Status Solidi A* **189**, 701 (2002)
- ¹²J. Shen, Z. Gai, and J. Kirschner, *Surf. Sci. Rep.* **52**, 163 (2004).
- ¹³H.-U. Krebs, *Int. J. Non-Equilib. Process.* **10**, 3 (1997)
- ¹⁴H. Jenniches, J. Shen, C. V. Mohan, S. S. Monoharan, J. Barthel, P. Ohresser, M. Klaua, and J. Kirschner, *Appl. Phys. Lett.* **69**, 3339 (1996).
- ¹⁵J. Shen, H. Jenniches, C. V. Mohan, J. Barthel, M. Klaua, P. Ohresser, and J. Kirschner, *Europhys. Lett.* **43**, 349 (1998).
- ¹⁶H. Jenniches, J. Shen, C. V. Mohan, S. S. Monoharan, J. Barthel, P. Ohresser, M. Klaua, and J. Kirschner, *Phys. Rev. B* **59**, 1196 (1999).
- ¹⁷M. Weinelt, S. Schwarz, H. Baier, S. Müller, L. Hammer, K. Heinz, and Th. Fauster, *Phys. Rev. B* **63**, 205413 (2001)

- ¹⁸M. Bloch, *J. Appl. Crystallogr.* **18**, 33 (1985)
- ¹⁹R. Feidenhans'l, *Surf. Sci. Rep.* **10**, 105 (1989)
- ²⁰I. K. Robinson and D. J. Tweet, *Rep. Prog. Phys.* **55**, 599 (1992)
- ²¹I. K. Robinson *Phys. Rev. B* **33**, 3830 (1986)
- ²²We use the primitive surface (s) setting of the unit cell, which is related to the face centered setting of the bulk (b) by the following relations: $[100]_s = 1/2 \times ([100]_b - [010]_b)$, $[010]_s = 1/2 \times ([100]_b + [010]_b)$, and $[001]_s = [001]_b$
- ²³E. Vlieg, *J. Appl. Crystallogr.* **30**, 532 (1997)
- ²⁴ R_u is defined as $R_u = \sum |F_{\text{obs}}| - |F_{\text{calc}}| / \sum |F_{\text{obs}}|$, where F_{obs} and F_{calc} are the observed and calculated structure factors, respectively, and the summation runs over all datapoints; for the definition of the GOF see Refs. 19,20
- ²⁵C. Boeglin, H. Bulou, J. Hommet, X. Le Cann, H. Magnan, P. Le Fèvre, and D. Chandesris, *Phys. Rev. B* **60**, 4220 (1999)
- ²⁶S.-K. Lee, J.-S. Kim, B. Kim, Y. Cha, W. K. Han, H. G. Min, J. Seo, and S. C. Hong, *Phys. Rev. B* **65**, 014423 (2001)
- ²⁷H. L. Meyerheim (unpublished).
- ²⁸J. Burchhardt, E. Lundgren, M. M. Nielsen, J. N. Andersen, and D. L. Adams, *Surf. Rev. Lett.* **3**, 1339 (1996)
- ²⁹S. H. Kim, H. L. Meyerheim, J. Barthel, J. Kirschner, J. Seo, and J. S. Kim, *Phys. Rev. B* **71**, 205418 (2005)
- ³⁰N. A. Levanov, V. S. Stepanyuk, W. Hergert, D. I. Bazhanov, P. H. Dederichs, A. A. Katsnelson, and C. Massobrio, *Phys. Rev. B* **61**, 2230 (2000).
- ³¹V. S. Stepanyuk, A. L. Klavskyuk, L. Niebergall, A. M. Saletsky, W. Hergert, and P. Bruno, *Phase Transitions* **78**, 61 (2005).
- ³²K. Wildberger, V. S. Stepanyuk, P. Lang, R. Zeller, and P. H. Dederichs, *Phys. Rev. Lett.* **75**, 509 (1995).
- ³³The potentials are used in the form of Ref. 30. The parameters are the following for Co-Co: $A^1=0.0$ eV, $A^0=0.1275$ eV, $\xi = 1.5105$ eV, $p=12.0136$, $q=1.9661$, $r_0=2.4042$ Å; for Co-Pd: $A^1=-0.7686$ eV, $A^0=-0.091$ eV, $\xi=0.7932$ eV, $p=8.439$, $q = 3.696$, $r_0=2.7948$ Å, for Pd-Pd: the same as in V. Rosato *et al.*, *Philos. Mag. A* **59**, 321 (1989).
- ³⁴T. Hoshino, W. Schweika, R. Zeller, and P. H. Dederichs, *Phys. Rev. B* **47**, 5106 (1993)